ioMosaic®
Minimizing risk. Maximizing potential.®

Analysis of PRV Stability In Relief Systems Part II

Screening

An ioMosaic® Publication

G. A. Melhem, Ph.D., FAIChE

IOMOSAIC® CORPORATION

Analysis of PRV Stability In Relief Systems Part II
Screening

Process Safety and Risk Management Practices

authored by

G. A. Melhem, Ph.D., FAIChE

Printed October 18, 2024

Notice:

This document was prepared by ioMosaic® Corporation (**ioMosaic**) for Public Release. This document represents ioMosaic's best judgment in light of information available and researched prior to the time of publication.

Opinions in this document are based in part upon data and information available in the open literature, data developed or measured by ioMosaic, and/or information obtained from ioMosaic's advisors and affiliates. The reader is advised that ioMosaic has not independently verified all the data or the information contained therein. This document must be read in its entirety. The reader understands that no assurances can be made that all liabilities have been identified. This document does not constitute a legal opinion.

No person has been authorized by ioMosaic to provide any information or make any representation not contained in this document. Any use the reader makes of this document, or any reliance upon or decisions to be made based upon this document are the responsibility of the reader. ioMosaic does not accept any responsibility for damages, if any, suffered by the reader based upon this document.

Revision Log:

Revision 1: January 3, 2022
Revision 2: September 25, 2024

...

Table of Contents

List of Figures

List of Tables

1 Introduction

In part I [7] of this paper we established a detailed dynamics methodology for the modeling of PRV stability. We demonstrated that (a) the irrecoverable inlet pressure loss due to friction has essentially no impact on PRV stability (also see [8]), (b) PRV instability is caused by the coupling of PRV disk motion with the pressure wave caused by excessive acoustic pressure drop (1/4 wave) during PRV opening/closing, (c) the instability does not amplify, and (d) liquid systems are the most likely to cause damage to piping and piping components.

In this paper we provide a simplified model for the assessment of PRV stability where the inlet line geometry is simple and/or where the inlet line acoustic length can be established. This simplified model has also been proposed in the 3rd ballot of API-520 part II.

2 Simple Model Parameters

PRV stability is heavily influenced by the inlet and discharge piping configuration. Excessive inlet pressure loss or backpressure can cause PRV chatter and/or flutter. As the PRV starts to open, the pressure upstream of the PRV starts to decrease due to sudden expansion. This gives rise to an expansion wave that will travel upstream. As the expansion wave reaches the pressure source (Vessel) upstream, it reflects and travels back towards the PRV as a compression wave. The largest upstream pressure fluctuations are expected to occur during fast opening or closing of the PRV. The interaction of the pressure wave and valve opening/closing can cause instability. Note that during the opening of the PRV, a delay is typically observed in backpressure buildup because of the time needed to fill body-bowl and the discharge piping. Body-bowl choking and backpressure can influence the force balance on the disk and as a result can cause instability.

In order to apply the simple screening model we need to establish the speed of sound in the inlet line, the PRV opening and closing times, and the acoustic pressure drop associated with PRV opening/closing.

2.1 Speed of Sound Estimates [1]

The speed of sound values used in the estimation of wave travel time can be subject to uncertainty. This is most important for liquids and two-phase systems. The piping flexibility can lower the value of the speed of sound. The presence of small amounts of entrained gas in liquids can also reduce the speed of sound. Adding a small amount of gas to a liquid, say 0.01 % by weight can lower the speed of sound for the two-phase mixture by as much as a factor of two. Note that the two-phase speed of sound depends on the change of vapor quality (flash fraction) with pressure, temperature, and composition. Flashing flow speed of sound values can be as low as 10 or 15 m/s.

The speed of sound, c_0, characterizes the propagation of an infinitesimal pressure wave in a fluid that is unconfined. The effective speed of sound, c, of a fluid confined by an elastic tube wall depends on both the fluid properties and the pipe elasticity.

For rigid piping, the speed of sound is equal to the fluid speed of sound:

$$c = c_0 = \sqrt{\frac{1}{\kappa_S \rho}} = \sqrt{\left[\frac{\partial P}{\partial \rho}\right]_s} = \sqrt{\frac{C_p}{C_v}\frac{1}{\kappa_T \rho}} = \sqrt{\frac{C_p}{C_v}\left[\frac{\partial P}{\partial \rho}\right]_T} \tag{1}$$

where κ_S is the isentropic compressibility, ρ is the fluid mass density, κ_T is the isothermal compressibility, C_p is the real fluid heat capacity at constant pressure and C_v is the real fluid heat capacity at constant volume. For liquids where C_p is approximately equal to C_v, the speed of sound can be approximated by:

$$c_0 \simeq \sqrt{\left[\frac{\partial P}{\partial \rho}\right]_T} \tag{2}$$

For piping that is anchored against longitudinal movement throughout its length:

$$c = c_0 \eta = \frac{c_0}{\sqrt{1 + \frac{E_f}{E_s}\frac{d}{\delta}\left(1 - \nu^2\right)}} \tag{3}$$

Where $E_f = \frac{1}{\kappa_T}$ is the fluid isothermal bulk modulus of elasticity [1] in Pa, E_s is the pipe material of construction modulus of elasticity in Pa, d/δ is the piping diameter to thickness ratio, and ν is Poisson's ratio ($\simeq 0.3$). An equation of state is typically used to calculate the fluid compressibility factors since this data is not readily available for all fluids and especially for mixtures.

For piping anchored against longitudinal movement at the upper end:

$$c = c_0 \eta = \frac{c_0}{\sqrt{1 + \frac{E_f}{E_s}\frac{d}{\delta}\left(1.25 - \nu\right)}} \tag{4}$$

For piping where frequent expansion joints are present:

$$c = c_0 \eta = \frac{c_0}{\sqrt{1 + \frac{E_f}{E_s}\frac{d}{\delta}}} \tag{5}$$

The impact of piping flexibility on speed of sound estimates is illustrated in Table 1 for steel piping with frequent expansion joints. The speed of sound reduction is most important for liquids that are highly incompressible where thin wall piping is used.

The various equations used above for the effective speed of sound c are typically expressed in one form as shown by Equation 5 because the values of $1 - \nu^2$ and $1.25 - \nu$ are approximately one. As the value of $\frac{E_f}{E_s}\frac{d}{\delta}$ tends towards a value of 10, the ratio of c/c_0 tends towards 0.3 as shown in Figure 1.

[1] The adiabatic bulk modulus of elasticity can also be used. $E_f = \frac{1}{\frac{C_v}{C_p}\kappa_T} = \frac{C_p}{C_v}\frac{1}{\kappa_T} = \frac{C_p}{C_v}E_T$

Table 1: Impact of piping flexibility on speed of sound reduction

Material	Piping Schedule US	E_f, GPa	$\frac{d}{\delta}$	η
Liquid Water	5	2.19	52.2	0.799
Liquid Water	10	2.19	35.5	0.850
Liquid Water	40	2.19	13.4	0.934
Liquid Water	80	2.19	11.3	0.944
Liquid Water	160	2.19	6.47	0.967
Liquid Propane	5	0.11	52.2	0.986
Liquid Propane	10	0.11	35.5	0.991
Liquid Propane	40	0.11	13.4	0.996
Liquid Propane	80	0.11	11.3	0.997
Liquid Propane	160	0.11	6.47	0.998
Vapor Propane	5	6.8×10^{-4}	52.2	1.000
Vapor Propane	10	6.8×10^{-4}	35.5	1.000
Vapor Propane	40	6.8×10^{-4}	13.4	1.000
Vapor Propane	80	6.8×10^{-4}	11.3	1.000
Vapor Propane	160	6.8×10^{-4}	6.47	1.000

Propane data at 293 K and 8.35 bara

2.2 Estimation of K_s and m_D

Grolmes [2] has recently developed an empirical method for the estimation of spring constants (K_s) and weights in motion (m_D) based on actual measurements of several PRVs and associated components. His measurements included a 4P6 and a 6Q8 as well smaller valves as shown in Table 2.

Note that the weight in motion reported by Grolmes [2] includes 1/3 of the spring mass (see Figure 2. Grolmes provides the following equation for the estimation of the PRV spring constant:

$$K_s = C_1\left[\frac{P_{set}A_N}{x_{max}}\right] = \underbrace{C_2C_3}_{C_1}\left[\frac{P_{set}A_N}{x_{max}}\right] = \underbrace{\left(\frac{P_{full\,flow}}{P_{set}}\right)}_{C_2}\underbrace{\left(\frac{A_{pop}}{A_N}\right)}_{C_3}\left[\frac{P_{set}A_N}{x_{max}}\right] \tag{6}$$

where C_1, C_2, and C_3 are dimensionless constants close to 1 in magnitude. He also provides an empirical formula for estimating the weight in motion:

$$m_D = \frac{M_{PRV}}{100}\left(1.8 + 0.022M_{PRV}\right) = 0.018M_{PRV} + 0.00022M_{PRV}^2 \tag{7}$$

where M_{PRV} is the valve body weight in pounds including a 150 # flange. The actual spring constants calculated by Grolmes [2] as shown in Table 2 were calculated using the following equation:

$$K_s = \frac{Gd}{8C^3N_a} = \frac{Gd}{8C^3\left(N_t - 2\right)} = \frac{E}{2\left(1+\nu\right)}\frac{d}{8C^3\left(N_t-2\right)} \tag{8}$$

Table 2: PRV constants measured by Grolmes

	Consolidated Dresser	Consolidated Dresser	Farris	Farris	Farris	Consolidated Dresser	Crosby
Model	1906Fc	1905Fc	26FA10	26GA10L	26PB10-120	1910-30-Qc	
Serial Number	TJ46345	TH85105	67041-A10	545342-1-A14/G	7511-A9	TC78912	
Bellows	No	No	No	No	Yes	Yes	
Inlet - in	1	1	1	1	4	6	6
Flange	300# RF	150# RF	150# RF	150# RF	150# RF	300# RF	
Outlet - in	2	2	2	2	6	8	6
Flange	150# RF	150# RF	150# RF	150# RF	150# RF	150# RF	
Nozzle [Letter]	F	F	F	G	P	Q	M
API Area - in^2	0.307	0.307	0.307	0.503	6.38	11.05	
Set Pressure - psig	100	120	180	100	50	185	$\simeq$ 2385
Name Plate Rating	695 scfm air	818 scfm air	1239 scfm air	145 usgpm water	7932 scfm air		
Catalog Rating	698 scfm air	821 scfm air	1239 scfm air	145 usgpm water	7877 scfm air	43000	
Date of Manufacture	Oct-91	Jan-90		Oct-08			
Dead Weight - lb	43	39.5	38.5	39	185		
Catalog Weight - lb	45	45	44	50	190	530	
Redbook Nozzle Area - in^2	0.375	0.375	0.371	0.559	7.087	12.85	
Measured Nozzle Area - in^2	0.363	0.363	0.371	0.567	6.4108	12.347	3.40
Redbook Lift in	0.182	0.182	0.206	0.326	0.901	1.09	0.54
Measured:							
Spring Weight - g	103	112	360	241	2555.2	14968	
Cap and Bellows - g	322	322	96	231	3137.7	19731	
Spring Rod - g	269.5	230	205	126	513	2268	
Spring Button - g	51	51	107	103	731.7	5216	
Total Weight In motion - g	676.8	640.3	528.0	540.3	5234.1	32204.3	
Spring Free Length - in	2.737	2.000	4.1875	4.275	7.6875	12.125	
Spring OD - in	1.343	1.380	1.7620	1.605	3.5590	7.091	
Spring ID - in	0.960	0.975	1.1670	1.125	2.5120	4.875	
Spring Wire Diameter - in	0.192	0.202	0.2975	0.240	0.5250	1.108	
Spring Check - in	-0.001	0.000	0.0000	0.000	-0.0015	0.0000	
Spring Pitch - in	0.407	0.413	0.4670	0.486	0.9750	2.25	
Spring Coil Angle - Degrees	8.0	8.0	9.0	7.0	9.0	9.0	
Spring G - psi	1.16×10^7	1.16×10^7	1.16×10^7	1.16×10^7	1.16×10^7	1.18×10^7	
Spring Mean Diameter - in	1.1515	1.1775	1.4645	1.365	3.0355	5.983	
Spring C or D/d	6.00	5.83	4.92	5.69	5.78	5.40	
Spring Active Coils - #	5.7	3.8	8.0	7.8	6.9	4.4	
K_s - lbf/in	225	385	454	243	572	2365	16380
K_s - N/m	39474	67383	79478	42483	100166	414119	2868543
m_D - kg	0.677	0.640	0.528	0.540	5.234	32.204	27.2
f_n - Hz	38.4	51.6	61.7	44.6	22.0	18.0	51.68
Estimated:							
$\frac{A_D}{A_N}$	1.3	1.3	1.3	1.3	1.3	1.2	
$\frac{A_D}{A_{bel}}$					$\simeq$ 1.17	$\simeq$ 1.08	
K_s - lbf/in	289	347	455	241	552	2827	
K_s - N/m	50654	60785	79695	42155	96685	494925	
m_D - kg	0.677	0.612	0.499	0.680	5.171	31.253	
f_n - Hz	43.54	50.14	63.61	39.62	21.76	20.03	
Glide Surface Area - in^2	5.77	5.77	2.38	2.00	16.27	49.14	
Cap/Nozzle Impact Area - in^2	0.169	0.169	0.075	0.201	1.12	2.686	
m_D / Valve Weight - %	3.32	3.14	2.64	2.39	6.07	13.40	

Crosby 6M6 was reported by Langerman [9]

Figure 1: Sonic velocity as a function of tube wall modulus of elasticity

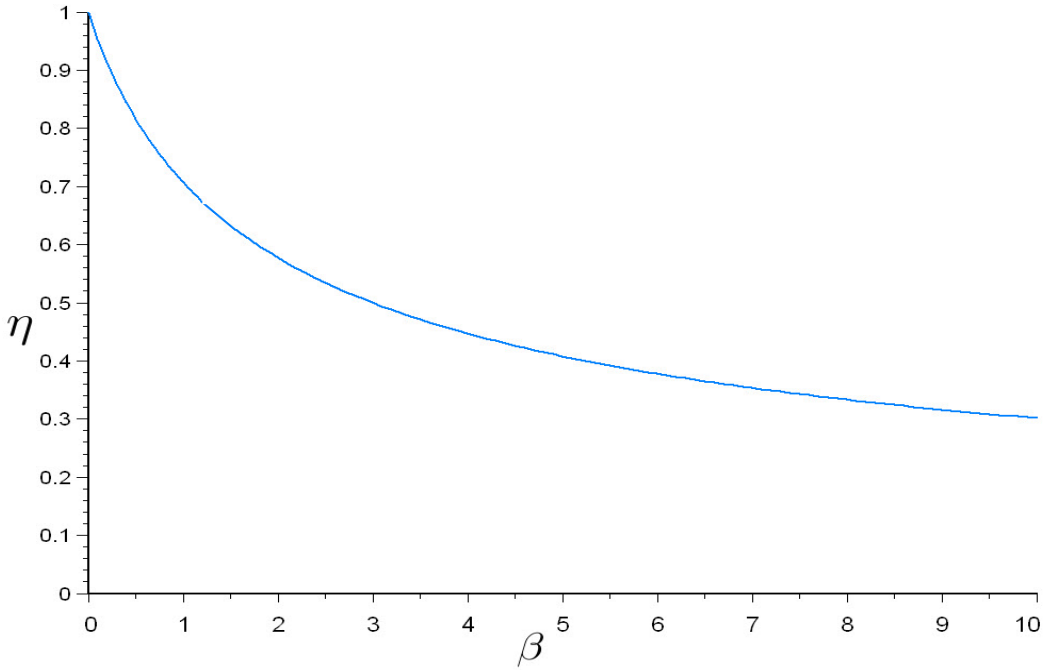

where d is the wire diameter, N_a is the number of active coils, C is the diameter modulus ($\frac{D}{d}$), D is the mean diameter, G is the modulus of torsion, E is Young's modulus of elasticity and $\nu \simeq 0.3$ is Poisson's ratio (see Figure 3). Note that E and G change with temperature as shown in Figure 4.

Once K_s and m_D are known, using a single degree of freedom model (SDOF) we can calculate the undamped natural frequency of the valve:

$$\tau_n = \frac{2\pi}{\omega_n} = 2\pi\sqrt{\frac{m_D}{K_s}} \tag{9}$$

$$f_n = \frac{1}{\tau_n} = \frac{\omega_n}{2\pi} = \frac{1}{2\pi}\sqrt{\frac{K_s}{m_D}} \tag{10}$$

where ω_n is the undamped circular natural frequency in $\mathrm{radians/s}$, τ_n is the undamped natural period in s, and f_n is the undamped natural frequency in Hz where one Hz equals 1 cycle/second.

2.3 PRV Opening and Closing Time

Once the spring constant and weight in motion are calculated, the PRV SDOF model can be used to establish the valve opening time. Grolmes [10] also provides a simple equation for the estimation of the PRV undamped opening time:

$$t_{open} \simeq \frac{1}{2\pi f_n}\sqrt{\frac{2}{A_{pop}/A_N - 1}} \simeq \frac{1}{2f_n} \tag{11}$$

Figure 2: Pressure Relief Valve Operation as a Spring-Mass System [2]

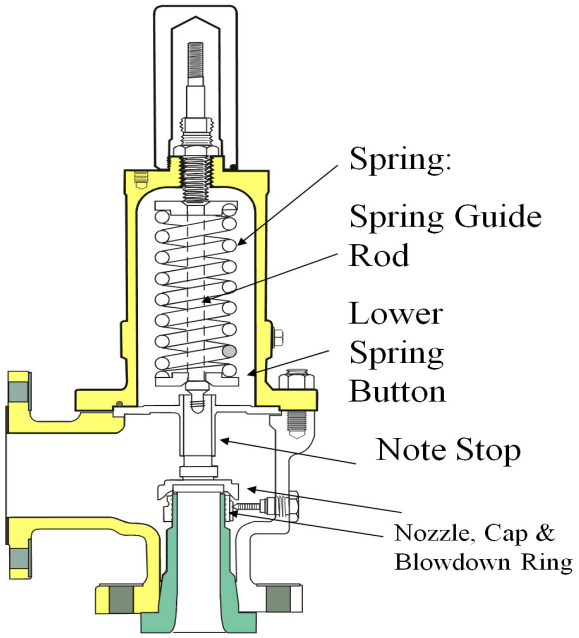

The mass is there, but not in one lump. There is the valve cap, a slider piece, the spring rod, a restraining button and some part of the spring itself. (1/3 total Spring Wgt.)

Figure 3: Helical Springs Constants [2]

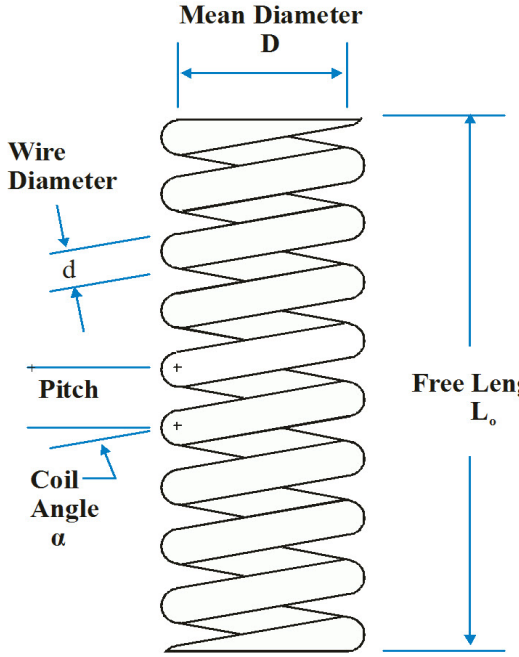

Relief Valves typically

have springs with closed ends ground such that the number of active coils is Na = Nt – 2

Where Nt is the total number of coils

Figure 4: Temperature dependency of modulus of elasticity for some common materials of construction [2]

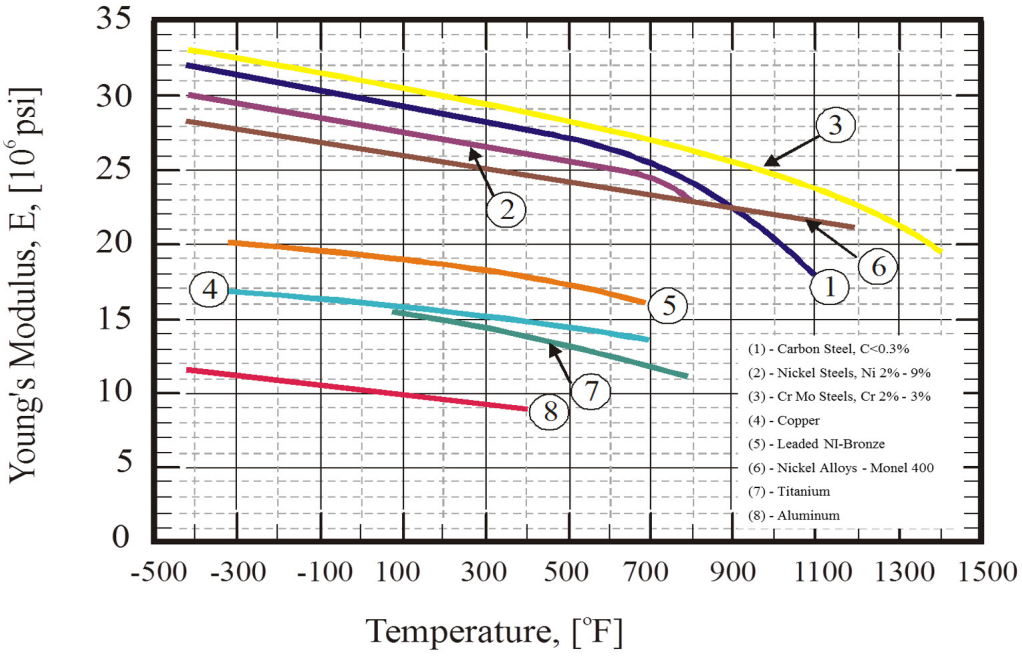

Recent analysis of the PERF-I data performed by Darby [4, 5, 6] suggest that the damping coefficient ζ that produced the best fit of the actual measurements of PRV opening ranged from 0.2 to 0.8 with the majority of the data well represented by a value around 0.5. The damped valve opening time can be approximated by:

$$t_{open,d} = \frac{t_{open}}{\sqrt{1-\zeta^2}} \tag{12}$$

At $\zeta = 0.5$, the damped opening time is equal to 1.15 times the undamped opening time. At $\zeta = 0.8$, the damped opening time is equal to 1.67 times the undamped opening time.

The PRV opening time depends strongly on the inlet pressure at the disk surface. A longer inlet line will lead to a lower pressure at the disk surface due to the higher value of acoustic pressure drop, and as a result a longer opening time. The opening time does not depend on the valve blowdown. In general, the PRV opening time decreases with increasing set pressure and increases with increasing PRV size.

The PRV closing time depends on blowdown. A lower blowdown will result in a faster closing time while a higher blowdown will result in somewhat longer closing time.

We can apply the formulas provided by Grolmes earlier along with information from the Redbook to estimate the PRV constants and opening time. This is illustrated in Tables 3, 4, and 5 for Crosby JOS style valves, Farris 2600 valves, and Consolidated 1900 valves. Pentair [2] measured the undamped natural frequency of a Crosby 2J3 at 250 psig set pressure to be 67.8 Hz. This value is consistent with the 58 Hz value calculated in Table 3.

[2]Paul, K., Personal communication, July 2014

Table 3: Calculated Crosby JOS Style PRV Constants and Undamped Opening Time

Nominal Size	Nominal Weight lbs	API Area in^2	Redbook Area in^2	Redbook Lift in	Critical Lift in	K_s 50 psig lbf/in	f_n 50 psig Hz	K_s 100 psig lbf/in	f_n 100 psig Hz	K_s 250 psig lbf/in	f_n 250 psig Hz
1D2	36	0.110	0.124	0.151	0.099	44	22 [23.2]	89	31 [16.4]	222	48 [10.4]
1E2	36	0.196	0.221	0.205	0.133	58	25 [20.2]	117	35 [14.3]	292	55 [9.0]
1.5F2	50	0.307	0.347	0.257	0.166	73	22 [22.5]	146	31 [15.9]	365	50 [10.1]
1.5G2.5	50	0.503	0.567	0.328	0.212	93	25 [19.9]	187	35 [14.1]	467	56 [8.9]
1.5H3	55	0.785	0.888	0.410	0.266	117	26 [19.0]	234	37 [13.5]	584	59 [8.5]
2J3	66	1.287	1.453	0.525	0.340	149	26 [19.2]	299	37 [13.5]	747	**58 [8.6]**
3K4	116	1.838	2.076	0.628	0.406	179	19 [26.9]	357	26 [19.0]	893	42 [12.0]
3L4	152	2.853	3.221	0.782	0.506	222	17 [30.0]	445	24 [21.2]	1112	37 [13.4]
4M6	201	3.600	4.065	0.878	0.569	250	14 [35.8]	500	20 [25.3]	1250	31 [16.0]
4N6	260	4.340	4.900	0.964	0.624	274	12 [42.7]	549	17 [30.2]	1372	26 [19.1]
4P6	270	6.380	7.205	1.169	0.757	333	12 [40.1]	666	18 [28.3]	1664	28 [17.9]
6Q8	481	11.05	12.47	1.539	0.996	438	8 [59.0]	875	12 [41.7]	2188	19 [26.4]
6R8	564	16.00	18.06	1.852	1.199	527	8 [62.4]	1053	11 [44.1]	2634	18 [27.9]
8T10	882	26.00	29.36	2.361	1.529	671	6 [84.4]	1343	8 [59.7]	3357	13 [37.7]

150 psi flange

[] Undamped valve opening time in milliseconds

Table 4: Calculated Farris 2600 Style PRV Constants and Undamped Opening Time

Nominal Size	Nominal Weight lbs	API Area in^2	Redbook Area in^2	Redbook Lift in	Critical Lift in	K_s 50 psig lbf/in	f_n 50 psig Hz	K_s 100 psig lbf/in	f_n 100 psig Hz	K_s 250 psig lbf/in	f_n 250 psig Hz
1D2	42	0.110	0.150	0.131	0.109	62	23 [21.7]	124	33 [15.4]	309	51 [9.7]
1E2	42	0.196	0.225	0.160	0.134	76	25 [19.6]	152	36 [13.9]	380	57 [8.8]
1.5F2	44	0.307	0.371	0.206	0.172	97	28 [17.9]	195	40 [12.7]	486	62 [8.0]
1.5G2.5	50	0.503	0.559	0.253	0.211	119	28 [17.6]	239	40 [12.5]	597	63 [7.9]
1.5H3	54	0.785	0.873	0.316	0.264	149	30 [16.6]	298	43 [11.8]	746	67 [7.4]
2J3	58	1.287	1.430	0.405	0.337	191	32 [15.5]	381	46 [10.9]	953	72 [6.9]
3K4	145	1.838	2.042	0.484	0.403	228	18 [28.5]	456	25 [20.1]	1139	39 [12.7]
3L4	145	2.853	3.170	0.603	0.502	284	20 [25.5]	568	28 [18.0]	1419	44 [11.4]
4M6	190	3.600	4.000	0.677	0.564	319	17 [30.2]	638	23 [21.3]	1595	37 [13.5]
4N6	190	4.340	4.822	0.743	0.619	350	17 [28.8]	701	25 [20.4]	1752	39 [12.9]
4P6	190	6.380	7.087	0.901	0.751	425	19 [26.1]	849	27 [18.5]	2124	43 [11.7]
6Q8	345	11.05	12.27	1.186	0.988	559	13 [38.5]	1117	18 [27.2]	2793	29 [17.2]
6R8	345	16.00	17.78	1.427	1.189	673	14 [35.1]	1346	20 [24.8]	3364	32 [15.7]
8T10	600	26.00	28.94	1.821	1.518	858	10 [51.8]	1716	14 [36.6]	4291	22 [23.2]

150 psi flange

[] Undamped valve opening time in milliseconds

Table 5: Calculated Consolidated 1900 Style PRV Constants and Undamped Opening Time

Nominal Size	Nominal Weight lbs	API Area in^2	Redbook Area in^2	Redbook Lift in	Critical Lift in	K_s 50 psig lbf/in	f_n 50 psig Hz	K_s 100 psig lbf/in	f_n 100 psig Hz	K_s 250 psig lbf/in	f_n 250 psig Hz
1D2	40	0.110	0.128	0.110	0.101	63	24 [20.9]	126	34 [14.8]	314	54 [9.3]
1E2	40	0.196	0.228	0.147	0.135	84	28 [18.1]	167	39 [12.8]	419	62 [8.1]
1.5F2	45	0.307	0.357	0.182	0.169	106	29 [17.4]	212	41 [12.3]	529	64 [7.8]
1.5G2.5	55	0.503	0.585	0.234	0.216	135	28 [17.7]	270	40 [12.5]	675	63 [7.9]
1.5H3	60	0.785	0.913	0.292	0.270	169	30 [16.8]	338	42 [11.9]	844	66 [7.5]
2J3	75	1.287	1.496	0.374	0.345	216	29 [17.5]	432	40 [12.4]	1080	64 [7.8]
3K4	110	1.838	2.138	0.446	0.412	259	23 [21.4]	518	33 [15.1]	1294	52 [9.6]
3L4	140	2.853	3.317	0.556	0.514	322	21 [23.3]	644	30 [16.5]	1611	48 [10.4]
4M6	185	3.600	4.186	0.625	0.577	362	18 [27.7]	723	26 [19.6]	1808	40 [12.4]
4N6	220	4.340	5.047	0.685	0.634	398	16 [30.6]	796	23 [21.7]	1989	36 [13.7]
4P6	260	6.380	7.417	0.830	0.768	483	16 [32.2]	965	22 [22.8]	2413	35 [14.4]
6Q8	430	11.05	12.85	1.090	1.011	637	11 [44.1]	1273	16 [31.2]	3183	25 [19.7]
6R8	495	16.00	18.60	1.290	1.217	779	11 [45.4]	1557	16 [32.1]	3893	25 [20.3]
8T10	620	26.00	28.62	1.680	1.509	920	10 [51.6]	1840	14 [36.5]	4600	22 [23.1]

150 psi flange

[] Undamped valve opening time in milliseconds

Table 6: API/PERF Measured PRV Opening Times [4, 5, 6]

Valve Size	Opening Time at 50 psig, ms	Opening Time at 250 psig, ms
1E2	20.6 - 27.9	7.6 - 11.0
2J3	21.3 - 31.9	13.8 - 15.9
3L4	25.1 - 51.7	16.1 - 24.2

According to Consolidated [11], on average 1700-S (steam) valves should be assumed to open in 45 milliseconds. Additionally, large 6 inch valves will have an opening time of 55 milliseconds and smaller 1.5 inch valves will have an opening time of 35 milliseconds. Testing and analysis of relief device opening times conducted by the UK Health and Safety Executive (UK HSE) shows that 2H3 and 3K4 relief devices opened in as little as 5 milliseconds under very high overpressure [12, 13]. The UK HSE work was focused on examination of the effect of relief device opening times on transient pressures developed within liquid filled shells. Kruisbrink [14] found based on modeling of safety and relief valves in water hammer computer codes that the valves open on average in 25 milliseconds.

Data published recently [4, 5, 6] on valve opening time measurements conducted by API/PERF in 2005 confirm earlier statements and calculations regarding opening times. 1E2, 2J3, and 3L4 pressure relief valves were tested with nitrogen at pressures of 50 and 250 psig. The opening times are shown in Table 6.

Cremers et al. [15] published a simple formula to approximate the valve opening time based on their review of manufacturer literature and the data provided in reference [16]. Their formula depends on the valve flow area and set pressure and is applicable for valve nozzle flow diameters

Table 7: Calculated API/PERF Pressure Relief Valves Opening Times Using Equation 13

Valve Size	Opening Time at 50 psig, ms	Opening Time at 250 psig, ms
1E2	27.5 [20.6 - 27.9]	18.3 [7.6 - 11.0]
2J3	35.0 [21.3 - 31.9]	20.2 [13.8 - 15.9]
3L4	39.3 [25.1 - 51.7]	21.4 [16.1 - 24.2]

[] Measured by API/PERF

$\geq \frac{1}{2}$ inch:

$$t_{open} = \left[15 + 20\frac{\sqrt{2D_N}}{\left(\frac{P_{set}}{P_{atm}}\right)^{2/3}\left(1-\frac{P_{atm}}{P_{set}}\right)^2}\right]\left[\frac{x}{x_{max}}\right]^{0.7} \tag{13}$$

where t_{open} is the pressure relief valve opening time in milliseconds, D_N is the pressure relief valve nozzle flow diameter in inches, x is the actual lift, and x_{max} is the pressure relief valve maximum lift. If we apply equation 13 to calculate the pressure relief valve opening time for the API/PERF [4, 5, 6] 3L4 set at 50 psig, we calculate the following:

$$t_{open} = 15 + 20 \times \frac{\sqrt{2 \times 1.906}}{\left(\frac{64.7}{14.7}\right)^{2/3}\left(1-\frac{14.7}{64.7}\right)^2} = 15 + 20 \times \frac{1.952}{2.685 \times 0.597} = 39.4 \text{ ms} \tag{14}$$

This value is within the measured range of 25.1 to 51.7 ms. If we apply equation 13 to all three API/PERF pressure relief valves at 50 and 250 psig set points we obtain the following opening times as shown in Table 7.

Excellent predictions are obtained with the exception of the 1E2 at 250 psig which has a nozzle flow diameter of 1/2 inch which is at the lower limit of the equation applicability.

3 Proposed API-520 Engineering Analysis Simple Force Balance

API-520 part II includes a simplified form of the force balance developed by Melhem [7]. This simplified form can be used to establish if a specific PRV installation will behave in a stable manner once it is flowing, i.e. if the PRV will close prematurely due to excessive inlet pressure drop. For a conventional spring loaded PRV:

$$P_{\text{source}} - \Delta P_{f,wave} - \Delta P_{\text{wave}} - \Delta P_{\text{back}} > P_{\text{close}} \tag{15}$$

$$\left(1 + \frac{\%OP}{100}\right) P_{\text{set}} - \Delta P_{f,wave} - \Delta P_{\text{wave}} - P_{\text{back}} > \left(1 - \frac{\%BD}{100}\right) P_{\text{set}} \tag{16}$$

$$100\left(\frac{\Delta P_{\text{back}} + \Delta P_{f,wave} + \Delta P_{\text{wave}}}{P_{\text{set}}}\right) < \%BD + \%OP \tag{17}$$

$$\%BP + \%FPL + \%WPL + < \%BD + \%OP \tag{18}$$

This simple balance can be corrected if the PRV disk is protected from backpressure with bellows. Typically the bellows only protect 90 % of the disk surface due to manufacturing tolerance, therefore only 10 % of the backpressure is realized:

$$100\left(\frac{0.1\Delta P_{\text{back}}+\Delta P_{f,wave}+\Delta P_{\text{wave}}}{P_{\text{set}}}\right) \quad < \quad \%BD+\%OP \tag{19}$$

$$\frac{\%BP}{10}+\%FPL+\%WPL+ \quad < \quad \%BD+\%OP \tag{20}$$

In the absence of advanced tools such as SuperChems™ Expert (a component of Process Safety Office®) to establish the dynamics of pressure wave interaction with the valve disk, we can obtain a conservative estimate of ΔP_{wave} from acoustic wave theory. For simple piping configurations (constant diameter piping without area changes and/or the presence of other acoustic barriers) the upstream pressure drop or rise during the PRV opening or closing (fast opening or pop action assumed when valve goes into full open position) can be estimated from the following equations:

$$\begin{aligned}
t_{wave} &= \frac{2L_p}{c_0} \\
\tau &= \min\left(\frac{t_{wave}}{t_{valve}},1\right) \\
\Delta P_{wave} &= \underbrace{\tau\frac{c_0\dot{M}_{\text{close}}}{A_p}}_{\text{Fluid Hammer Term}} + \underbrace{\tau^2\frac{\dot{M}^2_{\text{close}}}{2\rho_0 A_p^2}}_{\text{Fluid Inertia Term}} \qquad 0\le\tau\le 1 \\
\Delta P_{wave} &= \tau\rho u c_0\left[1+\frac{\tau\rho u}{2\rho_0 c_0}\right] \quad 0\le\tau\le 1
\end{aligned} \tag{21}$$

where the subscript 0 indicates upstream vessel conditions, $\dot{M}_{\text{close}}$ is the mass flow rate during closing (a fraction of the mass flow rate at full PRV lift) and t_{valve} is the PRV opening or closing time. The fluid inertia term in ΔP_{wave} is normally small but becomes important for high speed flow where the pressure drop is severe and excessive.

For an ideal gas, the speed of sound $c_0 = \sqrt{\gamma\frac{P_0}{\rho_0}}$. Equation 21 is based on the acoustic wave theory where the valve opening or closing is assumed to be instantaneous. Singh and Shak [17] recommend the use of the steady state value of $\dot{M}$ as a conservative value during opening. During opening it is expected that the mass flow rate will be lower than the flow rate at full lift due to the pressure expansion causing the pressure at the surface of disk to drop rapidly. Likewise, the mass flow rate is expected to be lower than the full lift value as the valve starts to close. Singh and Shak measured values ranging from 60 % to 85 % of the mass flow rate at full lift. An average of 80 % is recommended to be used during closing with the API recommended simple force balance.

Similarly, the pressure drop due to friction during opening or closing of the PRV can be estimated from the steady state value and τ:

$$\Delta P_{f,wave}=\tau^2\Delta P_f=\tau^2\frac{\dot{M}^2\left(K+\frac{4fL_p}{D_p}\right)}{2\rho_0 A_p^2} \quad 0\le\tau\le 1 \tag{22}$$

where K is the number of velocity heads loss, f is the Fanning friction factor, D_p is the pipe diameter, and L_p is the pipe length. If the actual piping configuration is complex, one or two-dimensional fluid dynamics equations solutions may be required to estimate the acoustic pressure drop due to expansion and reflections of the pressure wave.

We have shown earlier [7] through detailed fluid dynamics that the wave pressure drop calculated from Equation 21 is accurate, especially for liquids. Equation 21 can be used to approximate the total pressure drop in the inlet relief line of a PRV installation as long as the inlet relief line geometry is simple. In previous examples [7] we have shown that once the valve is closed the calculated round trip travel time by the partial differential equations solution of the pressure wave is given by:

$$\Delta t = \frac{4L}{c_0} = \frac{4 \times 61}{1220} = 0.2 \text{ s} \tag{23}$$

This is also shown in Part I [7] Figure 5 in the expanded pressure-time profile which shows approximately 5 round trips for the pressure wave in 1 second once the valve is closed.

4 Validation of API Simple Force Balance

The API simple force balance described earlier is validated with the API/PERF measurements [4, 5, 6]. A total of 18 different PRV's were tested by API/PERF. 1E2, 2J3, and 3L4 PRVs were provided by three different manufacturers. Actual blowdowns and opening times for the PRVs were measured. Two different set pressures were used for the PRVs, 50 and 250 psig. The PRVs were tested with inlet piping of lengths of 2, 4, and 6 feet and no discharge piping.

Some PRVs were tested with both inlet and discharge piping at 50 psig. The discharge piping lengths selected resulted in a pressure drop of approximately 8 to 9 % of the set pressure of 50 psig. 31.4 ft was used for the 2J3 and 17.9 ft was used for the 3L4.

The simple API force balance is tested with the following parameters and conditions:

- Nitrogen test fluid
- Initial temperature = 25 C
- Initial pressure = 110 % of the set pressure
- Rigid piping, i.e. the speed of sound in nitrogen is not influenced by the inlet piping flexibility
- Inlet line fitting coefficient used was selected (approximately 0.2) to match the reported total inlet line pressure loss
- The PRV opening times (independent of blowdown) used were based on the measured values as shown in Table 6.

To apply the API force balance during closing of the PRV we need to establish the PRV closing time. Since this is a difficult number to establish without the use of dynamic simulation, we will

assume that the closing time is the same as the opening time (conservative) and we will use the upper value of the measured opening time for high blowdowns and the lower value of the measured opening time for the low blowdowns. As shown in Table 7 the upper measured opening times are very close to the predicted PRV opening times using Equation 13.

Table 8 shows the calculated force balance results vs. the PERF measured data for the 2J3 PRV. The closing time used for a set pressure of 50 psig is 31.9 ms and the closing time used for a set pressure of 250 psig is 13.8 ms. Table 9 shows the predictions for the 3L4 PRV and Table 10 shows the predictions for the 1E2 PRV.

The last column in Tables 8, 9 and 10 shows the calculated net force balance according to Equation 15. The ΔP_w column shows the calculated acoustic wave pressure drop using Equation 21. The column $\Delta P_{w,f}$ shows the calculated frictional component of the acoustic wave pressure drop using Equation 22. The column ΔP_o shows the calculated [%BP] backpressure in % for tests that used a discharge line. The column ΔP_i shows the calculated total inlet pressure drop and irreversible pressure drop [dPT/dPi]. All other data in the tables are measured data as reported by the various publications.

The simple API force balance performs well against the PERF data. Three false positives are calculated out of 44 data points. Note that the API force balance can also be applied during the opening phase of the PRV. In addition, since we established earlier that the PRV instability is quarter wave, we can augment the simple API force balance assessment by examining if the valve opening and/or closing time is approximately less (cycle), greater (flutter), or equal (instability) to $4L/c_0$ plus or minus a 20 % margin.

One should also note from the calculations that the frictional component of ΔP_{wave} is very small. This is consistent with the dynamics results [7] which indicate that frictional pressure drop has very little to do with PRV instability.

5 Step by Step Procedure for Calculation of the API Force Balance

This section illustrates a step by step procedure for calculation of the API simple force balance using the last data point from Table 8.

5.1 Step 1 - Calculate the PRV Opening/Closing Time

Equations 11 and 12 proposed by Grolmes can be used to estimate the PRV opening time after establishing the spring constant and weight in motion. The results for a 2J3 with a set point of 50 psig are shown in Tables 3, 4, and 5 for Crosby JOS style valves, Farris 2600 valves, and Consolidated 1900 valves. Assuming that the PRV is undamped, the opening time ranges from 15.5 to 19.25 ms. Assuming a damping factor of 0.5, the opening time ranges from 17.25 to 22.0 ms. These values are close to the lower value measured by API/PERF.

Table 8: Simple API force balance validation against PERF data. 2J3 PRV

Test No	P_{set} psig	BD %	L_i ft	ΔP_i %	ΔP_o %	ΔP_w psi	$\Delta P_{w,f}$ psi	Observed Behavior	Force Balance psi
16	250	5.6	2	1.9 [2.26 / 1.97]	0 [0]	20.627	0.196	Stable	18.178
10	250	6.4	2	1.9 [2.26 / 1.97]	0 [0]	20.627	0.196	Stable	20.178
4	250	7.6	2	1.9 [2.26 / 1.97]	0 [0]	20.627	0.196	Stable	23.178
15	50	11.8	2	2.3 [2.27 / 2.09]	8.5 [8.59]	1.98	0.008	Stable	4.616
15	50	11.8	4	3.4 [3.24 / 2.98]	8.5 [8.51]	3.977	0.045	Stable	2.625
15	50	11.8	6	4.5 [4.44 / 4.09]	8.5 [8.36]	5.968	0.139	Stable	0.612
9	50	9.1	2	2.3 [2.27 /2.09]	8.5 [8.59]	1.98	0.008	Stable	3.266
9	50	9.1	4	3.5 [3.24 /2.98]	8.5 [8.51]	3.977	0.045	Stable	1.275
9	50	9.1	6	4.6 [4.44 /4.09]	8.5 [8.36]	5.968	0.139	Stable	**-0.738**
3	50	8	2	2.2 [2.27 / 2.09]	8.5 [8.59]	1.98	0.008	Stable	2.716
3	50	8	4	3.2 [3.24 / 2.98]	8.5 [8.51]	3.977	0.045	Stable	0.725
3	50	8	6	4.3 [4.44 / 4.09]	8.5 [8.36]	5.968	0.139	Unstable	**-1.288**

[] Calculated

Alternatively, Equation 13 can be used to calculate the opening time at 100 % lift:

$$t_{open} = 15 + 20 \times \frac{\sqrt{2 \times 1.349}}{\left(\frac{64.7}{14.7}\right)^{2/3}\left(1 - \frac{14.7}{64.7}\right)^2} = 15 + 20 \times \frac{1.642}{2.685 \times 0.597} = 35.48 \text{ ms} \tag{24}$$

This value is very close the upper value measured by API/PERF.

In order to replicate the data shown in Table 8 we will use a value of 31.9 ms. The upper bound is appropriate since the measured blowdown in 8 %. When uncertainties exist, lower PRV opening or closing numbers will result in higher acoustic pressure drop and a more conservative screening analysis.

5.2 Step 2 - Calculate PRV Flow Capacity at 10 % Overpressure

The flow capacity of the system (6 ft inlet line, PRV, and 31.42 ft discharge line) is calculated at 0.94 kg/s. At this flow rate the backpressure is calculated at 8.36 % of the set point or 4.182 psi. The actual steady state total inlet line pressure loss is calculated to be 4.44 % of the set point and the irrecoverable inlet line pressure loss is calculated at 4.09 % of the set point.

Note that it is important to use the correct basis for PRV stability (inlet and outlet pressure loss) calculations. A common mistake is to use the allowable accumulation as a basis for both PRV capacity calculations and subsequent stability analysis. This is especially important for fire exposure scenarios where the allowable accumulation is 21%. For piping designed to meet the 3% rule at 10% overpressure, inlet pressure drop evaluated at 21 % overpressure is often found to be 3.2 to 3.5%, which is within the uncertainty margins of such calculations. However, this exceeds the

Table 9: Simple API force balance validation against PERF data. 3L4 PRV

Test No	P_{set} psig	BD %	L_i ft	ΔP_i %	ΔP_o %	ΔP_w psi	$\Delta P_{w,f}$ psi	Observed Behavior	Force Balance psi
18	250	4.40	2	1.8 [2.1 / 1.82]	0 [0]	17.766	0.133	Stable	18.102
18	250	4.40	4	2.7 [2.96 / 2.60]	0 [0]	35.99	0.762	Unstable	**-0.751**
12	250	5.70	2	1.8 [2.1 / 1.82]	0 [0]	17.766	0.133	Stable	21.352
6	250	11.90	2	1.8 [2.1 / 1.82]	0 [0]	11.737	0.059	Stable	42.955
6	250	11.90	4	2.7 [2.96 / 2.60]	0 [0]	23.619	0.337	Stable	30.795
17	50	10.60	2	2.5 [2.11 / 1.94]	8.5 [8.43]	1.229	0.003	Stable	4.855
17	50	10.60	4	3.5 [3.03 / 2.78]	8.5 [8.27]	2.459	0.016	Stable	3.69
17	50	10.60	6	4.6 [4.07 / 3.74]	8.5 [8.14]	3.685	0.048	Stable	2.498
11	50	5.60	2	2.3 [2.11 /1.94]	8.5 [8.43]	1.229	0.003	Stable	2.355
11	50	5.60	4	3.3 [3.03 / 2.78]	8.5 [8.27]	2.459	0.016	Stable	1.19
11	50	5.60	6	4.6 [4.07 / 3.74]	8.5 [8.14]	3.685	0.048	Stable	**-0.002**
5	50	4.30	2	2.3 [2.11 / 1.94]	8.5 [8.43]	1.229	0.003	Stable	1.705
5	50	4.30	4	3.3 [3.03 /2.78]	8.5 [8.27]	2.459	0.016	Stable	0.54
5	50	4.30	6	4.5 [4.07 / 3.74]	8.5 [8.14]	3.685	0.048	Stable	**-0.652**

[] Calculated

3% requirement considered by some organizations and enforcement agencies as a rigid criterion. Conversely, piping design to meet 21% built-up backpressure limitations at 21% overpressure, is found to exceed the 10% built-up backpressure when evaluated at rated capacity (10% overpressure). Results range from 15 to 20% built-up backpressure when evaluated at rated capacity.

5.3 Step 3 - Calculate Speed of Sound

We assume that the inlet piping is rigid and schedule 40. As a result the speed of sound for the fluid/piping system is equal to the speed of sound in the fluid or 352 m/s.

5.4 Step 4 - Calculate Acoustic Pressure Drop

The acoustic pressure drop is calculated using Equation 21. Note that the inlet pipe flow area is 0.002165 m^2 and the initial fluid density at 10 % overpressure and 25 C is 5.442 $\mathrm{kg/m}^3$. Also note that M_{close} is assumed to be at 80 % of the value at full lift as the PRV is closing as recommended

Table 10: Simple API force balance validation against PERF data. 1E2 PRV

Test No	P_{set} psig	BD %	L_i ft	ΔP_i %	ΔP_w %	$\Delta P_{w,f}$ psi	Observed Behavior	Force Balance psi
14	250	6.4	2	1.0 [1.17 / 1.02]	14.957	0.161	Stable	25.884
14	250	6.4	4	1.7 [1.83 /1.66]	30.284	1.042	Stable	9.675
14	250	6.4	6	2.2 [2.37 / 2.18]	45.940	3.079	Stable	**-8.018**
8	250	2.5	2	1.0 [1.17 / 1.02]	21.818	0.337	Stable	9.097
8	250	2.5	4	1.7 [1.83 /1.66]	44.506	2.183	Unstable	**-15.438**
8	250	2.5	6	2.3 [2.37 / 2.18]	49.074	3.491	Unstable	**-21.314**
2	250	5.6	2	1.0 [1.17 / 1.02]	21.818	0.337	Stable	16.847
2	250	5.6	4	1.7 [1.83 / 1.66]	44.506	2.183	Unstable	**-7.688**
2	250	5.6	6	2.2 [2.37 / 2.18]	49.074	3.491	Unstable	**-13.564**
13	50	9.9	2	1.1 [1.4 / 1.25]	1.394	0.006	Stable	8.551
13	50	9.9	4	1.9 [2.22 / 2.04]	2.793	0.04	Stable	7.118
13	50	9.9	6	2.7 [2.92 /2.71]	4.197	0.12	Stable	5.634
7	50	7.1	2	1.1 [1.40 / 1.25]	1.394	0.006	Stable	7.151
7	50	7.1	4	1.9 [2.22 /2.04]	2.793	0.04	Stable	5.718
7	50	7.1	6	2.6 [2.92 / 2.71]	4.197	0.12	Stable	4.234
1	50	5.3	2	1.2 [1.40 / 1.25]	1.893	0.011	Stable	5.747
1	50	5.3	4	2.0 [2.22 / 2.04]	3.802	0.074	Stable	3.776
1	50	5.3	6	2.7 [2.92 / 2.71]	5.726	0.220	Stable	1.706

[] Calculated

by Singh and Shak:

$$
\begin{aligned}
t_{wave} &= \frac{2L_p}{c_0} = 1000 \times \frac{2 \times 6 \times 0.3048}{352} = 10.4 \text{ ms} \\
\tau &= \min\left(\frac{t_{wave}}{t_{valve}}, 1\right) = \frac{10.4}{31.9} = 0.326 \\
\Delta P_{wave} &= \underbrace{\tau \frac{c_0 \dot{M}_{\text{close}}}{A_p}}_{\text{Fluid Hammer Term}} + \underbrace{\tau^2 \frac{\dot{M}^2_{\text{close}}}{2\rho_0 A_p^2}}_{\text{Fluid Inertia Term}} \qquad 0 \le \tau \le 1 \\
\Delta P_{wave} &= 0.326 \times \frac{352 \times 0.94 \times 0.8}{0.002165} + 0.326^2 \times \frac{0.94^2 \times 0.8^2}{2 \times 5.4 \times 0.002165^2} \\
&= 39,858 + 1187 \text{ Pa or } 5.95 \text{ psi}
\end{aligned}
\tag{25}
$$

The frictional component of the wave pressure drop is calculated using Equation 22 adjusting for M_{close}:

$$
\Delta P_{f,wave} = \tau^2 \Delta P_f = 0.326^2 \times 0.8^2 \times \frac{4.09 \times 50}{100} = 0.1388 \text{ psi} \tag{26}
$$

5.5 Step 5 - Calculate the Backpressure

This was calculated from the flow capacity of the PRV at 10 % overpressure to be 4.182 psi.

5.6 Step 6 - Calculate the API Simple Force Balance

The simple force balance can be calculated using Equation 15. At 8 % blowdown the reset pressure is calculated at 46 psig.

$$\begin{aligned} P_{\text{source}} - \Delta P_{f,wave} - \Delta P_{\text{wave}} - \Delta P_{\text{back}} &> P_{\text{close}} \text{ or} \\ 55 - 0.1388 - 5.95 - 4.182 - 46 &= -1.270 \text{ psi} \end{aligned}$$

This balance indicates that the PRV will behave in an unstable manner which is the reported measured behavior.

The same analysis can applied to the opening phase of the PRV.

$$\begin{aligned} P_{\text{source}} - \Delta P_{f,wave} - \Delta P_{\text{wave}} - \Delta P_{\text{back}} &> P_{\text{close}} \text{ or} \\ 55 - 0.216 - 7.515 - 4.182 - 46 &= -2.912 \text{ psi} \end{aligned}$$

6 PRV Flutter, Chatter, and Cycling Screening

Recent work by Chiyoda [18], Pentair [19] and ioMosaic [7] showed that PRV instability leading to flutter and/or chatter is due to the coupling of the PRV disk motion with the quarter wave pipe/fluid mode frequency without resonance. Izuchi [18] simplifies his detailed modeling analysis to restrict the inlet line length for stable PRV operation:

$$\alpha = \sqrt{\frac{x}{x + x_o}} \tag{27}$$

$$L \leq L_{crit} \tag{28}$$

$$L_{crit} = \frac{c\alpha}{4f_n} = \frac{c}{4f_n}\sqrt{\frac{x}{x + x_o}} \simeq \frac{\alpha}{2} c t_{valve} \tag{29}$$

where x_o is the initial compression of the PRV spring at zero lift in m, f_n is the damped PRV frequency in Hz, x is the PRV disk lift in m, L_{crit} is the critical inlet line length in m, α is a valve lift parameter, and c is the speed of sound in the fluid/pipe system in $\mathrm{m/s}$. x_o can be calculated from the set point of the PRV, the mass in motion, and the PRV spring constant:

$$x_o = \frac{P_{set} A_N - m_D g}{K_s} \tag{30}$$

where P_{set} is the set point in gauge pressure units, A_N is the PRV nozzle area, m_D is the PRV mass in motion and K_s is the spring constant.

As shown earlier, Grolmes [2] has recently developed an empirical method for the estimation of spring constants (K_s) and weights in motion (m_D) based on actual measurements of several PRVs and associated components.

$$K_s = C_1 \left[\frac{P_{set}A_N}{x_{max}}\right] = \underbrace{C_2 C_3}_{C_1} \left[\frac{P_{set}A_N}{x_{max}}\right] = \underbrace{\left(\frac{P_{full flow}}{P_{set}}\right)}_{C_2} \underbrace{\left(\frac{A_{pop}}{A_N}\right)}_{C_3} \left[\frac{P_{set}A_N}{x_{max}}\right] \tag{31}$$

where C_1, C_2, and C_3 are dimensionless constants close to 1 in magnitude. He also provides an empirical formula for estimating the weight in motion:

$$m_D = \frac{M_{PRV}}{100}\left(1.8 + 0.022 M_{PRV}\right) = 0.018 M_{PRV} + 0.00022 M_{PRV}^2 \tag{32}$$

where M_{PRV} is the valve body weight in pounds including a 150 # flange.

If we assume that m_D is small compared to $P_{set}A_N$, then we can approximate x_o by:

$$x_o = \frac{P_{set}A_N - m_D g}{\frac{P_{full}}{P_{set}}\frac{A_{pop}}{A_N}\frac{P_{set}A_N}{x_{max}}} \simeq \frac{P_{set}A_N}{\frac{P_{full}}{P_{set}}\frac{A_{pop}}{A_N}\frac{P_{set}A_N}{x_{max}}} \tag{33}$$

where x_{max} is the maximum PRV disk lift in meters. Typically $\frac{P_{full}}{P_{set}}$ is 1.1 and $\frac{A_{pop}}{A_N}$ ranges from 1.2 to 1.3 (say 1.3), we can further simplify Izuchi's stability criterion to the following:

$$\boxed{L \le L_{crit} = \frac{c}{4f_n}\sqrt{\frac{1.43x}{1.43x + x_{max}}}} \tag{34}$$

If the disk is at maximum lift, then the inlet line length should be limited to:

$$L \le L_{crit} = \frac{c}{4f_n}\sqrt{\frac{1.43x_{max}}{1.43x_{max} + x_{max}}} \le 0.77\frac{c}{4f_n} \tag{35}$$

At 60 % of maximum disk lift, the inlet line legnth requried for stable operation becomes:

$$\boxed{L \le L_{crit} = 0.68\frac{c}{4f_n}} \tag{36}$$

One can always solve for the actual PRV disk lift from a detailed force balance (see Melhem [7]) and calculate the required inlet line length for PRV stability in a more detailed manner. The expression above can be related to the PRV opening/closing time using Equation 11:

$$t_{valve} \simeq \frac{1}{2f_n} \tag{37}$$

$$\frac{2L}{c} \le \underbrace{\left(\sqrt{\frac{1.43\frac{x}{x_{max}}}{1.43\frac{x}{x_{max}} + 1}}\right)}_{\alpha} t_{valve} \tag{38}$$

$$L \le L_{crit} = \frac{\alpha}{2} c t_{valve} \tag{39}$$

Figure 5: Inlet Line Length Stability Limit as a Function of Disk Lift Ratio

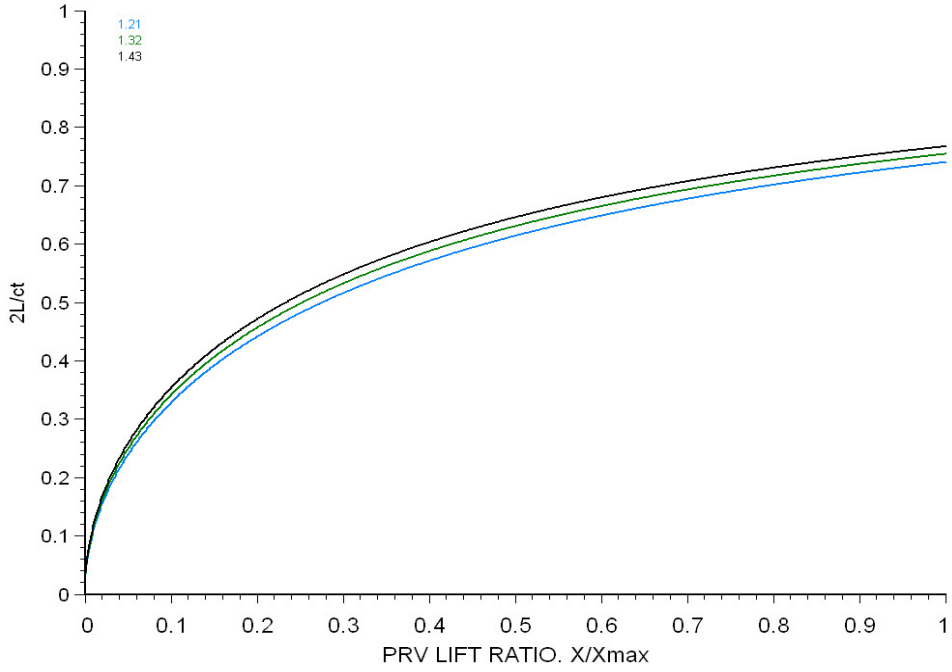

where α typically ranges from 0.68 to 0.77 (for A_{pop}/A_N ranging from 1.2 to 1.3). This expression is approximately 30 % less than the acoustic length stability criteria provided in the recently published API-520 part II in Appendix C.

If we plot $\frac{2L}{ct_{valve}}$ vs. $\frac{x}{x_{max}}$ at three different ratios of A_{pop}/A_N we get the behavior shown in Figure 5. The critical length criteria proposed by Chiyoda (Izuchi) [18] is very consistent with the critical length criteria proposed by Pentair [19]. This is illustrated in Figure 6. The Pentair measured experimental data are shown as open circles and X symbols [20]. The Pentair analytical critical length model is superimposed over the measured data in green. The red line represents the critical length criteria developed by Chiyoda (Izuchi) [18].

If we use the last data point from Table 8 to illustrate quarter wave screening procedure assuming a value of A_{pop}/A_N of 1.20, or $\alpha = 1.32$.

$$\frac{2L}{ct_{valve}} = \frac{2 \times 6 \times 0.3048}{352 \times 0.0319} = 0.33 \tag{40}$$

The critical disk lift ratio can be read from Figure 5 or calculated from:

$$\frac{x}{x_{max}} = \frac{0.33^2}{1.32\,(1 - 0.33^2)} = 0.0925 \tag{41}$$

As illustrated in Figure 6, the 3 % irreversible inlet pressure loss rule is not sufficient to guarantee PRV stability. The simplified API force balance discussed earlier can be extended to include the simplified quarter wave stability criteria.

Figure 6: Inlet Line Length Stability Limit Predictions for 2J3 PRV vs. Measured Data by Pentair

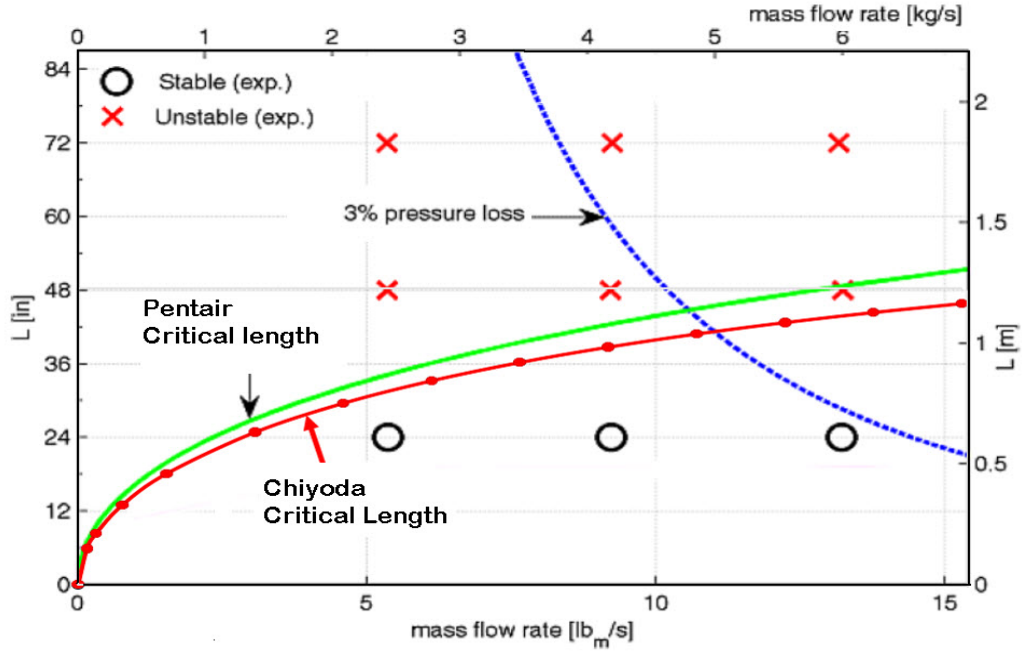

6.1 Enhanced Screening Criteria using Critical Length

Using the critical length criteria developed by Chyioda [18] and/or Pentair with their simplified models we can enhance the API PRV stability criteria. It should first be noted that in the initial opening or final closing stages of the PRV as the pressure rises from set pressures to 10 % over-pressure and vice versa, there is still the possibility of instability even though the PRV can become stable at the required flow capacity. It should also be noted that actual field PRV tests have shown that non-modulating pop action PRVs can operate stably at reduced lift.

Izuchi [3] introduces the concept of non-dimensional inlet line length, ϕ, which is the ratio of the valve natural frequency divided by the acoustic natural frequency of the 1st mode for the pipe/fluid system, or the duration of the pressure wave propagation (round trip) divided by the natural period of the valve disk/spring system:

$$\phi = \frac{f_n}{f_p} = \frac{2 f_n L}{c} \tag{42}$$

When the inlet line is longer than the critical inlet line length, higher acoustic modes can be excited (3/4 wave, 5/4 wave, 7/4 wave, ...). However, if the inlet line is much longer than the critical line length, $L >> \phi \frac{c}{2 f_n} >> \phi c t_{valve} >> \frac{2\phi}{\alpha} L_{crit} >> \sim 10 L_{crit}$, acoustic coupling is not likely to occur due to inreased damping effects. In this case, low frequency cycling will occur. More damping occurs with higher disk lift [3], i.e. more flow. Izuchi [3] illustrates the value of the required multiple of L_{crit} as a function of non-dimensional inlet pressure drop as shown in Figure 7.

This was also demonstrated experimentally by Izuchi [3] and by dynamic modeling of liquid systems by Melhem [7]. Izuchi [3] shows that an inlet line length of 10 m equal to 12.5 times the

Figure 7: Critical length multiplier as a function of non-dimensional inlet pressure drop [3]

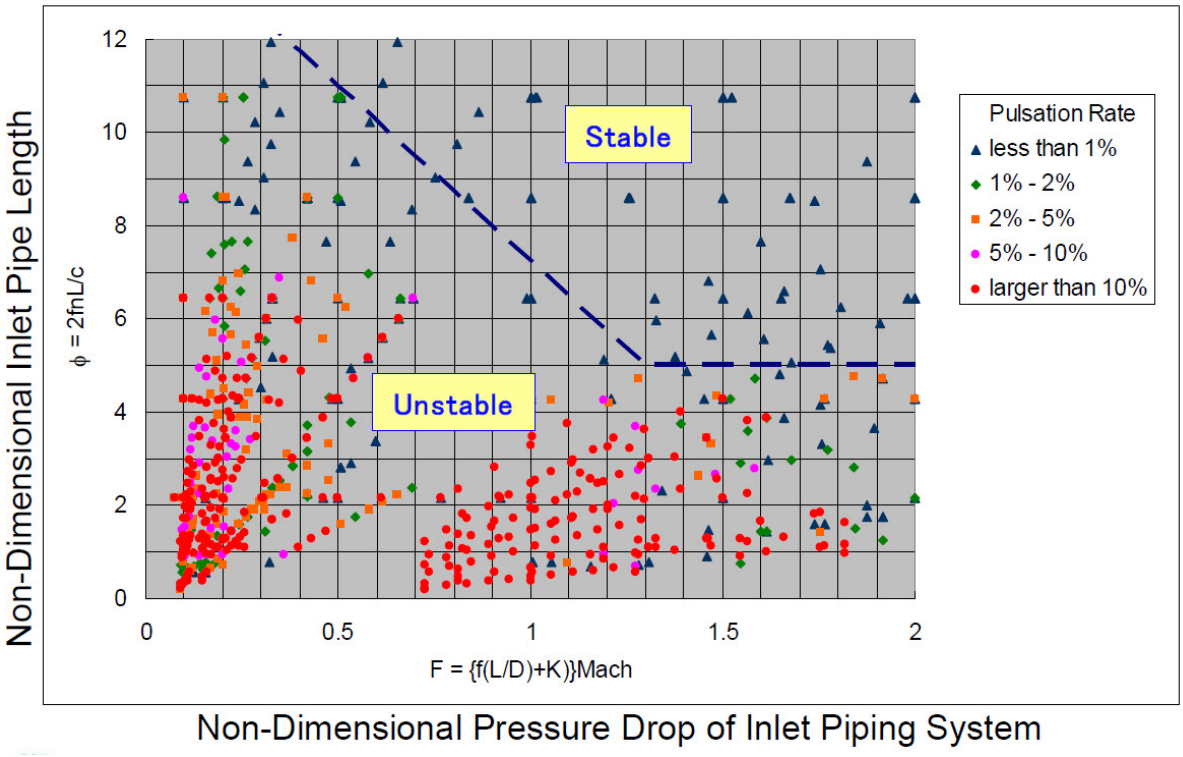

Figure 8: Critical length multiplier PRV stability guidance

$L \leq 0.8\ L_{crit}$	$L > 0.8\ L_{crit}$	$L > 1.2\ L_{crit}$	$L > 5 \sim 10\ L_{crit}$
No ¼ wave coupling	Strong ¼ wave coupling	High Frequency Cycling	Low Frequency Cycling

When the inlet line is less than the critical line length, L_{crit}, coupling of the valve disk motion with the pressure wave caused by valve closing/opening is not expected. This can lead to flutter if the disk force balance is negative.

When the inlet line is within 20 % of the critical line length, L_{crit}, strong coupling of the valve disk motion with the pressure wave caused by valve closing/opening is expected and can lead to chatter if the disk force balance is negative.

When the inlet line is greater then 1.2 times critical line length, L_{crit}, cycling is expected where the valve disk contacts the seat but at a lower frequency than that of the valve. This can lead to high frequency cycling when the disk force balance is negative which may not be tolerable.

When the inlet line is much greater then 1.2 times critical line length, L_{crit}, say 10 or 15 times the critical length, cycling is expected where the valve disk contacts the seat but at a much lower frequency than that of the valve. This can lead to cycling when the disk force balance is negative which is typically tolerable.

Figure 9: Enhanced Stability Screening Benchmarking Results

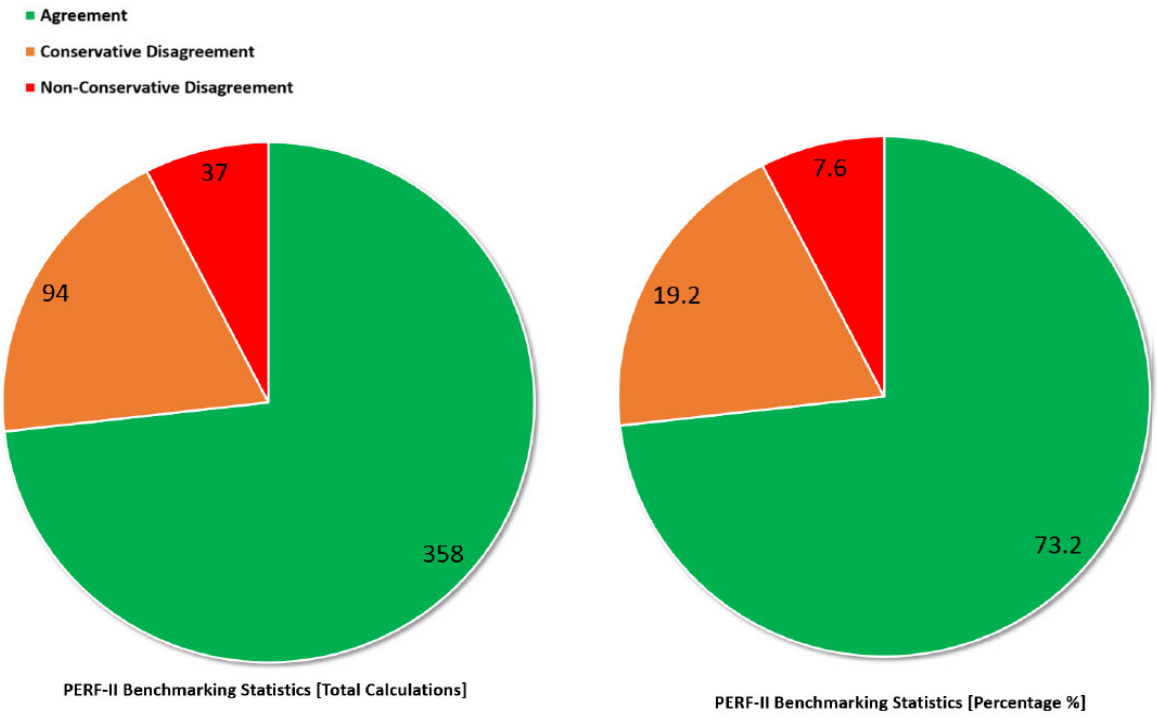

critical line length of 0.8 m [3]resulted in stable valve operation for gas flow while a line length of 5 m or 6.3 times the critical line length of 0.8 m resulted in chatter. Melhem [7] also shows stable operation for a liquid system when the inlet line length became longer than 15 meters for a critical line length of 7 m.

A critical length stability guidance as shown in Figure 8 can be used in conjunction with the force balance for simple screening of PRV stability. The enhanced screening methodology consisting of the force balance and critical line length stability criteria was benchmarked against several measured data sets with gas, liquid, and two-phase discharges. Figure 9 shows the benchmarking results with good agreement of predicted vs. observed/measured stability behavior. The data sets include measurements obtained by PERF-I [4, 5, 6], Chiyoda [3], the Electric Power Research Institute (EPRI) [16], and Bayer [21]. The benchmarking also includes numerous data sets from actual installations. The criteria applied in the benchmarking for low frequency cycling (stable) when the inlet line length is much longer than the critical length is 5 times the critical length.

Stability Screening:

First evaluate the API simple force balance at 10 % overpressure and full lift. If the force balance is positive than the PRV is **completely stable**. Note the API simplified force balance relies on a user specified blowdown, whereas the detailed static force balance requires specific valve SDOF model parameters. If the detailed static balance is used instead, one should ensure that the dynamic blowdown predictions are the same as the actual specified or expected PRV blowdown. The possi-

[3] f_n = 75 Hz, $t_{open} = \frac{1}{2f_n} = \frac{1}{150} = 0.0067$ s, c = 300 m/s, $L_{crit} = \frac{0.8ct_{open}}{2} = 0.8$ m

bility of instability would remain in the initial opening or final closing during short duration if the inlet line length is greater than the critical one.

If the force balance is negative at 10 % overpressure, reduce the PRV lift until the required flow capacity is reached. If the force balance is positive at the required capacity reduced lift and the reduced lift is larger than 30 % than the PRV is **stable at required capacity**. The possibility of instability would remain in the initial opening or final closing during short duration if the inlet line length is greater than the critical one.

If the force balance is negative at the reduced PRV lift required flow capacity and the inlet line length is less than the critical length, then the source pressure will continue to increase upstream until the force balance is positive at this reduced lift. The PRV is then unstable until the pressure reaches the level required to keep the force balance positive at the critical inlet line length. In this case the pressure at the upstream vessel would be higher than the 10 % overpressure though the PRV becomes stable at the final balanced position.

If the force balance is negative at the reduced PRV lift required flow capacity and the inlet line length is greater or equal to the critical inlet line length, then the PRV can be **Unstable**. It should be noted that when the inlet line length is much larger than the critical length (See test data by Izuchi [18] and dynamic modeling results by Melhem [7]) the PRV can operate in a stable manner. The worst condition for instability, **chatter**, occurs when the inlet line length is approximately equal to the critical length.

For gas service unstable motion in the initial opening or final closing would be permissible generally. For liquid and high pressure gas services unstable motion in the initial and final closing would not be permissible since the pressure fluctuation becomes so large that the piping damage or loosening of bolts might occur.

7 Conclusions

The existing 3 % inlet pressure loss rule is not sufficient to guarantee PRV stability. The proposed simple screening model in this paper takes into account all the key critical parameters that have been shown by detailed modeling and experiment to influence PRV stability. Benchmarks against several measured data sets show excellent performance. Critical to the performance of both the simple and detailed dynamic models are the PRV parameters (opening and closing times). These critical parameters must either be estimated using the methods described in this paper or provided by the PRV manufacturers.

8 Appendix A

Regardless of what model is used to calculate PRV stability, accurate values of the spring constant K_s and mass in motion, m_D are needed. Most operating companies maintenance shops will have the ability to disassemble a pressure relief valve and to measure what is needed to get an accurate estimate of K_s and m_D.

For example, the measurement methods used by Grolmes [2] when he developed his empirical formula are standard shop techniques. Grolmes used a set of good micrometers, calipers and inside depth gauges. He also used some rugged but accurate Ohaus Laboratory balance scales for the small parts and for the large valves he used some big spring scales that were accurate to +/- 1 lb. A sample Table listing information to be obtained and measured is shown in Table 11.

8.1 Weight In Motion

For the weight in motion measurement, the mass of all moving components will need to be weighed (see Figure 2):

- **Spring**: This is the total spring weight divided by 3.
- **Cap**: This is the ”disk” plus the ”disk holder” or ”disk retainer” as well as the ”slider” as shown in Figure 2. As measured by Grolmes, there is the cap or disk itself plus a disk holder that is sometimes referred to as the ”huddle chamber. This is what gives the lift augmentation effect. Then there is a slider element that moves inside of a guide cylinder. The slider moves and the guide does not. The ”slider” element may also be referred to as the ”stem retainer”. In his publications Grolmes included all of the cap related elements that move with the cap under ”cap and bellows” as shown in Table 2.
- **Bellows**: Grolmes’s original data included two entries for large valves that have bellows. The cap weight listed by Grolmes for those valves consists of all of the preceding cap elements plus the bellows. Grolmes did not or could not separate out the bellows as a separate element of weight because it is welded to the top of the cap as it should be to give the cap its backpressure isolation. If the bellows weight can be measured separately, it should be considered to be a spring with one end fixed and therefore only 1/3 of its weight is in motion. Note that the bellows spring constant should also be calculated and used in conjunction with the actual spring constant.
- **Spring Rod**: Some manufacturers may call this component a ”spindle” or a ”stem”. Every valve has a spring rod or spindle or stem. It is obvious in every manufacturer’s valve illustration. The full weight of this element is in motion. These are not trivial elements in large valves and should be measured and counted.
- **Spring Button**: Some manufacturers refer to this as ”spring washer” or ”spring plate”. In all the valves examined by Grolmes there was a Spring Button at the bottom of the spring. This is a centering element for the spring. There is a button at both ends of the spring. Only the bottom button is in motion and should be counted.

Table 11: K_s and m_D Data Measurement Requirements

General Information:		PRV A	PRV B	PRV C
Model				
Serial Number				
Bellows (Y/N)				
Inlet - in & Flange Rating				
Outlet - in & Flange Rating				
Nozzle [Letter] & API Area - in^2				
Set Pressure - psig				
Name Plate Flow Rating				
Date of Manufacture				
M_{PRV}, Dead Weight - lb				
A_N, Measured Nozzle Flow Area - in^2				
x_{max}, Measured Maximum Lift, in				
Weight In Motion Measurements:				
1/3 Spring Weight - g				
1/3 Bellows Weight - g				
Disk Weight - g				
Disk Holder Weight - g				
Slider Weight - g				
Spring Rod (Spindle, or Stem) Weight - g				
Spring Bottom Button (washer or plate) Weight - g				
m_D, Total Weight In motion - g	Σ Weights above			
$\frac{m_D}{453.6 \times M_{PRV}} \times 100$ - %				
Spring Constant:				
L_o, Spring Free Length - in				
d, Spring Wire Diameter - in				
α, Spring Coil Angle - Degrees				
D, Spring Mean Diameter - in				
$C = \frac{D}{d}$, Spring Diameter Modulus				
N_t, Total Number of Spring Coils				
$N_a = N_t - 2$, Number of Spring Active Coils				
$G = \frac{E}{2(1+\nu)}$, Spring Modulus of Torsion - psi				
$K_s = \frac{Gd}{8C^3 N_a}$ - lbf/in				
Disk Geometry Measurements:				
A_D, Disk Area - in^2				
A_N, Nozzle Area - in^2				
A_{bel}, Bellows Area - in^2				

8.2 Spring Constant

The spring constant K_s (see Figure 3) can be be calculated from spring dimension measurements and the spring material modulus of torsion, G. The modulus of torsion can be calculated from the spring material modulus of elasticity, E, and Poisson's ratio, $\nu \simeq 0.3$.

8.3 Disk Geometry

Values of A_D, A_N, and A_{bel} can also be measured. Typical ratio values of A_D/A_N range from 1.2 to 1.3 while typical ratio values of A_{bel}/A_D are approximately 0.9 since the entire disk area cannot be all covered by bellows. The valve geometry is illustrated in Figure 10. Note that $A_D = \pi R_d^2$, $A_N = \pi R_N^2$, and $A_{bel} = \pi R_b^2$.

Figure 10: PRV Geometry

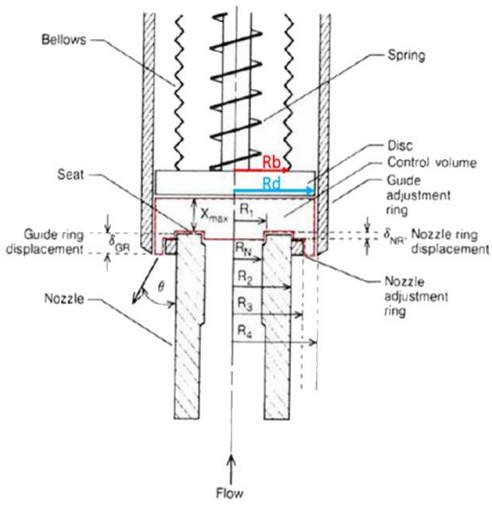

References

[1] G. A. Melhem. On the estimation of speed of sound and thermodynamic properties for fluid flow and PRV stability. In *DiERS Users Group Meeting*. DiERS, AIChE, April 2016.

[2] M. A. Grolmes. Odds and ends - relief valve stability - Part 4. In *DIERS Users Group Meeting*. American Society of Chemical Engineers, AIChE/DIERS, 2011.

[3] Hisao Izuchi. Chatter of safety valve. In *Presentation to API 520 Committee*. API, API, 2008.

[4] Ron Darby. The dynamic response of pressure relief valves in vapor or gas service - Part I: Mathematical model. *Journal of Loss Prevention in the Process Industries*, 26:1262–1268, 2013.

[5] A. A. Aldeeb, Ron Darby, and Scott Arndt. The dynamic response of pressure relief valves in vapor or gas service - Part II: Experimental investigation. *Journal of Loss Prevention in the Process Industries*, 2014.

[6] Ron Darby and A. A. Aldeeb. The dynamic response of pressure relief valves in vapor or gas service - Part III: Model validation. *Journal of Loss Prevention in the Process Industries*, 2014.

[7] G. A. Melhem. Analysis of PRV stability in relief systems. Part I - Detailed dynamics. *ioMosaic Corporation White Paper*, 2014.

[8] Kenneth Paul, Michael McNeely, Csaba Hos, and Alan Champneys. In *API 78th Fall Refining and Equipment Standards Meeting*. API, 2013.

[9] M. A. Langerman. An analytical model of a spring loaded safety valve. In *Testing and Analysis of Safety / Relief Valve Performance*, pages 55–63. American Society of Mechanical Engineers, ASME, 1983.

[10] M. A. Grolmes. Relief valve opening time estimation. CTI Note TN-11-580, 2011. Communicated June 27, 2011.

[11] Consolidated Safety Valves. Pressure drop considerations on pressure reliefvalve inlets. Technical Report CON/PI-10, Dresser Valve and Controls Division, 1988.

[12] Health and Safety Executive. Testing and analysis of relief device opening times. Technical Report Offshore Technology Report 2000/23, UK-HSE, 2002.

[13] Health and Safety Executive. Examination of the effect of relief device opening times on transient pressures developed within liquid filled shells. Technical Report Offshore Technology Report 2000/130, UK-HSE, 2000.

[14] A. C. Kruisbrink and H. Bournemouth. Modeling of safety and relief valves in water hammer computer codes. In *International Conference on Developments in Valves and Actuators for Fluid Control*, 1990.

[15] J. Cremers, L. Friedel, and B. Pallaks. Validated sizing rule against chatter of relief valves during gas service. *Journal of Loss Prevention in the Process Industries*, 14:261–267, 2001.

[16] Electric Power Research Institute. EPI PWR safety and relief valve test program: Safety and relief valve test report. Technical Report NP-2628-SR, EPRI, 1982.

[17] A. Singh and D. Shak. Modeling of a spring loaded safety valve. In *Testing and Analysis of Safety / Relief Valve Performance*, pages 63–70. American Society of Mechanical Engineers, ASME, 1983.

[18] Hisao Izuchi. Stability analysis of safety valve. In *10th Topical Conference on Gas Utilization*. AIChE, AIChE, 2010.

[19] C. J. Hos, A. R. Champneys, K. Paul, and M. McNeely. Dynamic behavior of direct spring loaded pressure relief valves in gas service: II reduced order modelling. *Journal of Loss Prevention in the Process Industries*, 36:1–12, 2015.

[20] K. Paul. Dynamic behavior of direct spring loaded pressure relief valves - a review of stability concerns. In *Spring DIERS Users Group Meeting, Houston, Texas*. DIERS, AIChE, 2016.

[21] S. Kostos and J. Kim. Stability tests. In *Spring DIERS Users Group Meeting, Hamburg, Germany*. DIERS, AIChE, 2011.

....

Index

About the Authors

Dr. Melhem is an internationally known pressure relief and flare systems, chemical reaction systems, process safety, and risk analysis expert. In this regard he has provided consulting, design services, expert testimony, incident investigation, and incident reconstruction for a large number of clients. Since 1988, he has conducted and participated in numerous studies focused on the risks associated with process industries fixed facilities, facility siting, business interruption, and transportation.

Prior to founding ioMosaic® Corporation, Dr. Melhem was president of Pyxsys Corporation; a technology subsidiary of Arthur D. Little Inc. Prior to Pyxsys and during his twelve years tenure at Arthur D. Little, Dr. Melhem was a vice president of Arthur D. Little and managing director of its Global Safety and Risk Management Practice and Process Safety and Reaction Engineering Laboratories.

Dr. Melhem holds a Ph.D. and an M.S. in Chemical Engineering, as well as a B.S. in Chemical Engineering with a minor in Industrial Engineering, all from Northeastern University. In addition, he has completed executive training in the areas of Finance and Strategic Sales Management at the Harvard Business School. Dr. Melhem is a Fellow of the American Institute of Chemical Engineers (AIChE) and Vice Chair of the AIChE Design Institute for Emergency Relief Systems (DiERS).

Contact Information

Georges. A. Melhem, Ph.D., FAIChE
E-mail. melhem@iomosaic.com

ioMosaic Corporation
93 Stiles Road
Salem, New Hampshire 03079
Tel. 603.893.7009, x 1001
Fax. 603.251.8384
web. www.iomosaic.com

How can we help?

Please visit www.iomosaic.com and www.iokinetic.com to preview numerous publications on process safety management, chemical reactivity and dust hazards characterization, safety moments, video papers, software solutions, and online training.

In addition to our deep experience in process safety management (PSM), chemical reaction systems, and the conduct of large-scale site wide relief systems evaluations by both static and dynamic methods, we understand the many non-technical and subtle aspects of regulatory compliance and legal requirements. When you work with ioMosaic® you have a trusted ISO certified partner that you can rely on for assistance and support with the lifecycle costs of relief systems to achieve optimal risk reduction and PSM compliance that you can evergreen. We invite you to connect the dots with ioMosaic®.

We also offer laboratory testing services through ioKinetic® for the characterization of chemical reactivity and dust/flammability hazards. ioKinetic® is an ISO accredited, ultramodern testing facility that can assist in minimizing operational risks. Our experienced professionals will help you define what you need, conduct the testing, interpret the data, and conduct detailed analysis. All with the goal of helping you identify your hazards, define and control your risk.

ioMosaic®
Minimizing risk. Maximizing potential.®

About ioMosaic Corporation

Our mission is to help you protect your people, plant, stakeholder value, and our planet.

Through innovation and dedication to continual improvement, ioMosaic has become a leading provider of integrated process safety and risk management solutions. ioMosaic has expertise in a wide variety of disciplines, including pressure relief systems design, process safety management, expert litigation support, laboratory services, training, and software development.

As a certified ISO 9001:2015 Quality Management System (QMS) company, ioMosaic offers integrated process safety and risk management services to help you manage and reduce episodic risk. Because when safety, efficiency, and compliance are improved, you can sleep better at night. Our extensive expertise allows us the flexibility, resources, and capabilities to determine what you need to reduce and manage episodic risk, maintain compliance, and prevent injuries and catastrophic incidents.

Consulting Services

- Asset Integrity
- Auditing
- Due Diligence
- Facility Siting
- Fault Tree/SIL Analysis
- Fire & Explosion Dynamics
- Incident Investigation, Litigation Support, and Expert Testimony
- Hydrogen Safety
- LNG Safety
- LPG Safety
- Pipeline Safety
- Process Hazard Analysis
- Process Engineering Design and Support
- Process Safety Management
- Relief and Flare Systems Design and Evaluation
- Risk Management Program Development
- Quantitative Risk Assessment
- Software Solutions
- Structural Dynamics
- Sustainability Reporting Support
- Technology Transfer Package Development
- Process Safety Training

Laboratory Testing Services (ISO Accredited)

- Battery Safety Testing
- Chemical Reactivity Testing
- Combustible Dust Hazard Analysis and Testing
- Flammability Testing
- Physical Properties Testing
- Process Safety Services
- Specialized Testing

US Offices

Salem, New Hampshire
Houston, Texas
Minneapolis, Minnesota
Berkeley, California

International Offices

Al Seef, Kingdom of Bahrain
Bath, United Kingdom

Software Solutions

Process Safety Office® : A suite of integrated tools for process safety professionals and risk analysts.

Process Safety Enterprise® : Process Safety Management compliance made easy with enterprise workflows, dynamic forms, document management, key performance indicators and metrics, and more.

Process Safety Learning® : Build your process safety competencies incrementally using learning modules.

Process Safety tv® : The worldś first video streaming platform dedicated to process safety.

Contact us

www.ioMosaic.com
sales@ioMosaic.com
1.844.ioMosaic